Conformational Memories and the Endocannabinoid Binding Site at the Cannabinoid CB1 Receptor

Judy Barnett-Norris,[†] Dow P. Hurst,[†] Diane L. Lynch,[†] Frank Guarnieri,[‡] Alex Makriyannis,[§] and Patricia H. Reggio*,[†]

Department of Chemistry and Biochemistry, Kennesaw State University, 1000 Chastain Road, Kennesaw, Georgia 30144, Sarnoff Corporation, 201 Washington Road, Princeton, New Jersey 08543, and School of Pharmacy, University of Connecticut, 372 Fairfield Road, Storrs, Connecticut 06269

Endocannabinoid stucture−activity relationships (SAR) indicate that the CB1 receptor recognizes ethanolamides whose fatty acid acyl chains have 20 or 22 carbons, with at least three homoallylic double bonds and saturation in at least the last five carbons of the acyl chain. To probe the molecular basis for these acyl chain requirements, the method of conformational memories (CM) was used to study the conformations available to an n-6 series of ethanolamide fatty acid acyl chain congeners: 22:4, n-6 ($K_i = 34.4 \pm 3.2$ nM); 20:4, n-6 ($K_i = 39.2 \pm 5.7$ nM); 20:3, n-6 ($K_i = 53.4 \pm 5.5$ nM); and 20:2, n-6 ($K_i > 1500$ nM). CM studies indicated that each analogue could form both extended and U/J-shaped families of conformers. However, for the low affinity 20:2, n-6 ethanolamide, the higher populated family was the extended conformer family, while for the other analogues in the series, the U/J-shaped family had the higher population. In addition, the 20:2, n-6 ethanolamide U-shaped family was not as tightly curved as were those of the other analogues studied. To quantitate this variation in curvature, the radius of curvature (in the C-3 to C-17 region) of each member of each U/J-shaped family was measured. The average radii of curvature (with their 95% confidence intervals) were found to be 5.8 Å (5.3−6.2) for 20:2, n-6; 4.4 Å (4.1−4.7) for 20:3, n-6; 4.0 Å (3.7−4.2) for 20:4, n-6; and 4.0 Å (3.6−4.5) for 22:4, n-6. These results suggest that higher CB1 affinity is associated with endocannabinoids that can form tightly curved structures. Endocannabinoid SAR also indicate that the CB1 receptor does not tolerate large endocannabinoid headgroups; however, it does recognize both polar and nonpolar moieties in the headgroup region. To identify a headgroup orientation that results in high CB1 affinity, a series of dimethyl anandamide analogues (*R*)-*N*-(1-methyl-2-hydroxyethyl)-2-(*R*)-methyl-arachidonamide ($K_i = 7.42 \pm 0.86$ nM), (*R*)-*N*-(1-methyl-2-hydroxyethyl)-2-(*S*)-methyl-arachidonamide ($K_i = 185 \pm 12$ nM), (*S*)-*N*-(1-methyl-2-hydroxyethyl)-2-(*S*)-methyl-arachidonamide ($K_i = 389 \pm 72$ nM), and (*S*)-*N*-(1-methyl-2-hydroxyethyl)-2-(*R*)-methyl-arachidonamide ($K_i = 233 \pm 69$ nM) were then studied using CM and computer receptor docking studies in an active state (R*) model of CB1. These studies suggested that the high CB1 affinity of the *R,R* stereoisomer is due to the ability of the headgroup to form an intramolecular hydrogen bond between the carboxamide oxygen and the headgroup hydroxyl that orients the C2 and C1′ methyl groups to have hydrophobic interactions with valine 3.32(196), while the carboxamide oxygen forms a hydrogen bond with lysine 3.28(192) at CB1. In this position in the CB1 binding pocket, the acyl chain has hydrophobic and C−H···π interactions with residues in the transmembrane helix (TMH) 2−3−7 region. Taken together, the studies reported here suggest that anandamide and its congeners adopt tightly curved U/J-shaped conformations at CB1 and suggest that the TMH 2−3−7 region is the endocannabinoid binding region at CB1.

Introduction

Anandamide (*N*-arachidonoylethanolamine, **1**; Chart 1), isolated from porcine brain, was first to be identified as an endogenous ligand of the G-protein-coupled cannabinoid CB1 receptor.[1] Like other cannabinoid agonists, **1** produces a concentration-dependent inhibition of the electrically evoked twitch response of the mouse vas deferens[1] as well as antinociception, hypothermia, hypomotility, and catalepsy in mice.[2] Anandamide

exhibits higher affinity for the cannabinoid CB1 receptor than for the CB2 receptor.[3] Two other polyunsaturated fatty acid ethanolamides, homo-γ-linolenylethanolamide (**2**) and 7,10,13,16-docosatetraenylethanolamide (**3**), have been isolated from porcine brain and shown to bind to the cannabinoid CB1 receptor with high affinity.[4] In addition, a fatty acid glycerol ester, *sn*-2-arachidonoyl-glycerol (2-AG; **4**)[5] and 2-arachidonyl glyceryl ether (**5**)[6] have been identified as endogenous cannabinoid ligands.

Anandamide−CB1 receptor interactions result in activation of G-proteins, particularly of the $G_{i/o}$ family.[7] Termination of anandamide signaling at the cannabinoid receptors occurs through an uptake mechanism that transports anandamide into the cell[8] where it
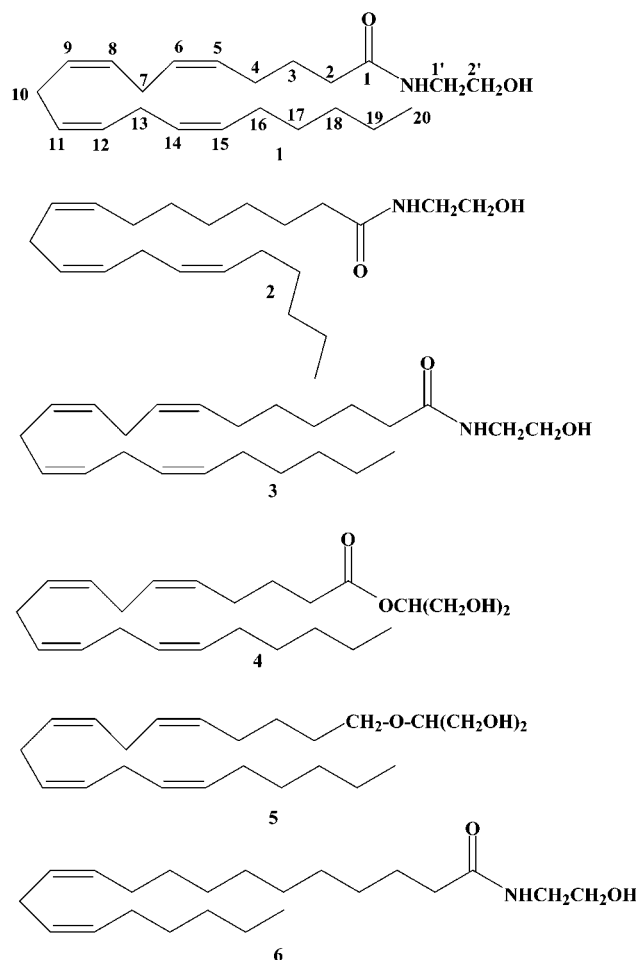
---

* To whom correspondence should be addressed. Tel: (770) 423-6170. Fax: (770) 423-6744. E-mail: preggio@kennesaw.edu.
† Kennesaw State University.
‡ Sarnoff Corporation.
§ University of Connecticut.

Chart 1

Table 1. Reported CB1 Affinities for Analogues 7−10

analogue	chirality		K_i (nM)[a]	analogue	chirality		K_i (nM)[a]
	C2	C1′			C2	C1′	
7	R	R	7.42 ± 0.86	**9**	S	S	389 ± 72
8	S	R	185 ± 12	**10**	R	S	233 ± 69

[a] CB1 binding data from Goutopoulos et al.[14]

subsequently undergoes rapid degradation by a membrane-bound amidohydrolase (called anandamide amidohydrolase or fatty acid amide hydrolase, FAAH), which has been cloned.[9]

Endocannabinoid structure−activity relationships (SAR) developed to date for binding to CB1 have focused upon ethanolamide derivatives and have recently been reviewed.[10,11] This SAR indicates that the CB1 receptor does not tolerate large endocannabinoid headgroups; however, it does recognize both polar and nonpolar moieties in the headgroup region.[10,11] The receptor recognizes ethanolamides whose fatty acid acyl chains have 20 or 22 carbons, with at least three homoallylic double bonds (i.e., at least three cis double bonds separated by methylene carbons) and saturation in at least the last five carbons of the acyl chain. This SAR is evidenced by the large decrease in CB1 affinity that results when the number of homoallylic double bonds drops below three as seen in the following n-6 series of ethanolamides reported by Sheskin and co-workers:[12] 22:4, n-6 (**3**, K_i = 34.4 ± 3.2 nM), 20:4, n-6 (**1**, K_i = 39.2 ± 5.7 nM), 20:3, n-6 (**2**, K_i = 53.4 ± 5.5 nM); and 20:2, n-6 (**6**, K_i > 1500 nM). Double-bond conjugation within the acyl chain results in diminished CB1 affinity as well.[10,11]

(*R*)-(+)-Arachidonyl-1′-hydroxy-2′-propylamide or *R*-methanandamide, in which a methyl group (with *R* stereochemistry) was introduced at C1′ in the headgroup of **1**, has 4-fold higher affinity for CB1 than **1** and resistance to hydrolysis by FAAH.[13] The introduction

of a methyl group at both C1′ in the headgroup and at C2 in the acyl chain resulted in compounds that exhibit high enantio- or diastereomeric preference for the CB1 receptor (**7−10**; see Table 1).[14] Binding studies revealed that an *R,R* substitution pattern resulted in a very high affinity anandamide analogue (**7**; K_i = 7.42 ± 0.86 nM). This analogue had 25-, 52-, and 31-fold higher CB1 affinity than its congeners, **8** (C2 *S*, C1′ *R*; K_i = 185 ± 12 nM), **9** (C2 *S*, C1′ *S*; K_i = 389 ± 72 nM), and **10** (C2 *R*, C1′ *S*; K_i = 233 ± 69 nM). These results suggest that the *R,R* stereochemistry orients the headgroup of anandamide in a very favorable position at the CB1 binding site.

In this paper, the method of conformational memories (CM)[15] is employed to identify both the acyl chain conformation adopted by an endocannabinoid ethanolamide at the CB1 binding site and the endocannabinoid headgroup orientation for maximum interaction at this same site. Information from these CM studies is then used to identify a specific binding site for endocannabinoid ethanolamides at the CB1 receptor. This binding site is shown to be consistent with both the endocannabinoid SAR literature and the cannabinoid CB1 receptor mutation literature and represents the first integration of all of these elements to describe the endocannabinoid/CB1 receptor complex in a three-dimensional (3D) context.

Results

Conformational Analysis Using CM. Conformational analysis of highly flexible ligands such as the endogenous cannabinoids is a challenging problem due to the large number of conformations available to the ligand. The most commonly used method in the literature for studying such flexible ligands has been molecular dynamics (MD).[16] However, MD techniques reveal short time molecular motion but are generally incapable of a complete exploration of the conformational space of flexible ligands. CM has been shown to achieve complete sampling of the conformational space of highly flexible molecules, to converge in a very practical number of steps and to be capable of overcoming energy barriers efficiently.[15] The program X-Cluster in Macromodel[17] is used to group the conformers generated by CM into families of like conformation called "clusters". In the work reported here, conformers were grouped using X-Cluster according to their increasing rms devia-
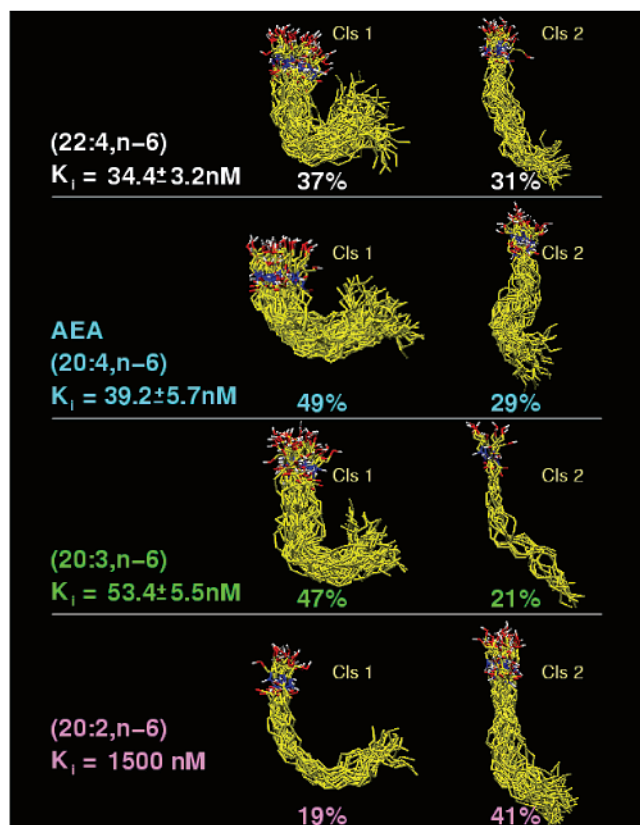
Figure 1. CM results in $CHCl_3$ are reported here for the major conformational families of the following ethanolamides: 22:4, n-6 (**3**); 20:4, n-6 (**1**); 20:3, n-6 (**2**); and 20:2, n-6 (**6**). Percentages reported here are the percentage populations out of 100 conformers generated in the final phase of the CM calculation at 310 K. CB1 K_i values listed here were reported by Sheskin et al.[12]

tion from the first structure output at 310 K. Because X-Cluster rearranges the conformers so that the rms deviation between nearest neighbors is minimized, any large jump in rms deviation is indicative of a large conformational change and hence identifies a new conformational family or clusters (Cls). Conformational families that are identified by CM to be highly populated are those that have low free energies, while conformations that outlie these major groupings are those whose free energies are not sufficiently low enough to be visited frequently during the simulation.

CM Analysis of Endocannabinoid Acyl Chain Conformations. In the C_{20}/C_{22} n-6 ethanolamide series, Sheskin and co-workers reported an abrupt decrease in CB1 affinity when the number of homoallylic double bonds decreased below three double bonds. Figure 1 illustrates the CM results for the n-6 series of ethanolamides (**1–3** and **6**) in $CHCl_3$. CM identified two major clusters for **1–3** and **6**, an extended shape cluster in which the ends of the molecule are far from each other and a curved cluster in which the ends of the molecule are brought closer together. For anandamide (**1**; 20:4, n-6; $K_i = 39.2 \pm 5.7$ nM), 49 out of 100 conformers were in a U shape (Cls 1) in which the four homoallylic double bonds form the curved portion of the U, bringing the head and tail close together. Twenty-nine out of 100 conformers of **1** (Cls 2) were in an extended conformation.

Table 2. Analogue K_i Cluster 1 Average Radius Curvature (Å)

analogue	K_i (nM)[a]	cluster 1 members	average radius curvative (Å) (95% confidence limit)
20:2, n-6 (**6**)	>1500	19 (16)[b]	5.8[c] (5.3−6.2)
20:3, n-6 (**2**)	53.4 ± 5.5	47 (42)	4.4 (4.1−4.7)
20:4, n-6 (**1**)	39.2 ± 5.7	49 (25)	4.0 (3.7−4.2)
22:4, n-6 (**3**)	34.4 ± 3.2	37 (28)	4.0 (3.6−4.5)

[a] CB1 binding data from Sheskin et al.[12] [b] The number in parentheses represents the number of structures used for analysis after elimination of outliers as described in the Materials and Methods section. [c] The radius of **6** was found to be statistically different from those of **1–3** by one way ANOVA analysis.

For **3** (22:4, n-6; $K_i = 34.4 \pm 3.2$ nM), 37 out of 100 conformers (Cls 1) also place the four homoallylic double bonds in the curved portion of the acyl chain, but because there are two additional carbons between the carboxamide carbon and the first double bond (i.e., C_{22} vs C_{20}), Cls 1 appears more J-shaped. Thirty-one out of 100 conformers of **3** (Cls 2) were in extended conformations.

For **2** (20:3, n-6; $K_i = 53.4 \pm 5.5$ nM), 47 out of 100 conformers (Cls 1) place the three homoallylic double bonds in the curved portion of the acyl chain. Because there is one less double bond (relative to **1**), there are two additional sp^3 hybridized carbons between the carboxamide carbon and the first double bond (at C8−C9); this portion of the acyl chain is extended, producing a J-shaped overall appearance. Twenty-one out of 100 conformers of **2** were in extended conformations.

For **6** (20:2, n-6; $K_i > 1500$ nM), 19 conformers out of 100 conformers formed a broad U-shaped cluster (Cls 1), while 41 out of 100 conformers were in extended conformations (Cls 2).

While it is clear from the CM results illustrated in Figure 1 that each analogue can form both extended and U/J-shaped families of conformers, these families differ in two important ways. First, for the 20:2, n-6 ethanolamide, the higher populated cluster is the extended conformer cluster (Cls 2), while for the other analogues in the series, the U/J-shaped cluster (Cls 1) has the higher population. Second, while the 20:2, n-6 ethanolamide has a curved cluster, this cluster is not as tightly curved as are those of the other analogues studied. Because the greatest differences in the CM results for the n-6 series were associated with the curved cluster (Cls 1), we hypothesized that the CB1 affinity differences seen in this series may be related to the tightness of curvature in the Cls 1 conformers.

To quantitate the tightness of curvature in the U/J-shaped cluster (Cls 1) of the acyl chain analogues (**1–3** and **6**), the radius of curvature of the acyl chain was determined by fitting a circle to each Cls 1 conformer in the region from C3 to C17 (see numbering system illustrated in Chart 1) and then calculating an average radius of curvature for each Cls 1, as well as a standard error. The results of this analysis are given in Table 2. Here, the numbers of members in Cls 1 for each analogue are shown, followed in parentheses by the number of conformers used in the curvature analysis. A discussion of the criteria for inclusion in the curvature analysis is provided in the Materials and Methods section.

The average radii of analogues (**1–3**) were found to be 4.0, 4.4, and 4.0 Å, respectively. These radii were not
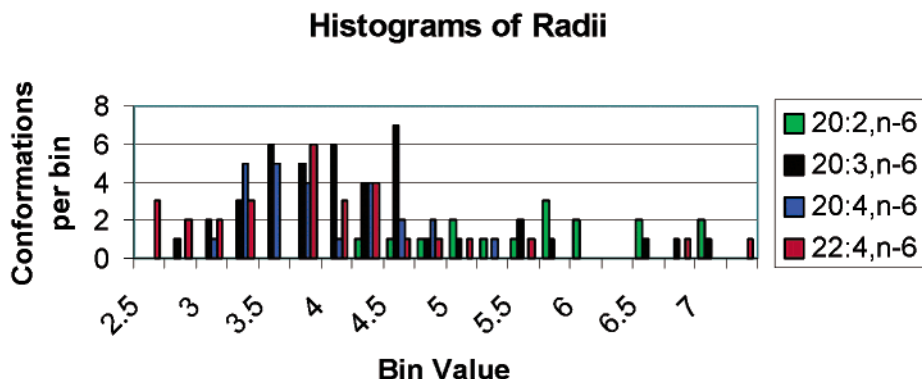
Histograms of Radii

Figure 2. Histogram of curvature radii data for the 20:2, n-6 (**6**); 20:3, n-6 (**2**); 20:4, n-6 (**1**); and 22:4, n-6 (**3**) analogues is provided here. The histogram was generated by counting the number of conformers in each 0.25 Å window, starting at a radius of 2.5 Å.

found to be statistically different from each other. The average radius of the 20:2, n-6 analogue (**6**; $r = 5.8$ Å) was larger than the radii of **1**−**3** and was shown to be statistically different (by one way analysis of variance (ANOVA)) from the radii of the other three analogues.[18] Figure 2 provides a histogram that illustrates how Cls 1 conformer radii are distributed for each acyl chain analogue. It is clear here that the curvature radii for Cls 1 of the 20:2, n-6 analogue (**6**) are shifted to higher values, indicating substantially lower curvature for this analogue as compared to Cls 1 of the 20:3, n-6 (**2**); 20:4, n-6 (**1**); or 22:4, n-6 (**3**) families. The radius of **6** was found to be statistically different from those of **1**−**3** by one way ANOVA analysis. These results suggest that higher CB1 affinity is associated with endocannabinoids that can form tightly curved structures.

CM Analysis of 7−10. A conformational analysis of **7**−**10** (see Table 1) in CHCl$_3$ was performed using the CM method. One hundred structures at 310 K were sampled and output in the final phase of the CM calculations for each analogue.

Headgroup. Figure 3 illustrates the CM results obtained in the AMIIIX series. This figure shows the headgroups of all 100 conformers of each compound superimposed at their amide groups. The methyl groups at the C2 (in green) and C1′ (in magenta) stereocenters are colored here. The acyl chains (colored in cyan) have been truncated in order to simplify the display. In Figure 3, the enantiomeric pairs **7/9** and **8/10** are positioned with the amide group nearly perpendicular to the page and the amide oxygen pointing up. In this orientation, it is clear that the CM results reflect that these pairs of compounds are enantiomers. It is also clear here that the C2 methyl (in green) and C1′ methyl (in magenta) groups can only populate a small portion of space and that the acyl chains (colored in cyan) have a preferred direction as they emerge from the head-group.

Acyl Chain Conformations in 7−10. While results illustrated in Figure 3 show that there is a preferred departure direction for the acyl chain in each stereo-isomeric pair, the general shapes of the acyl chain clusters were found to be similar to the acyl chain clusters previously identified for anandamide and 2-AG[19] and seen above in Figure 1 (20:4, n-6 analogue, **1**). This would be expected since **7**−**10** all have 20:4, n-6 acyl chains. Some deviation from CM results for **1**, Cls 1 was seen in the position of the last five carbons of the acyl
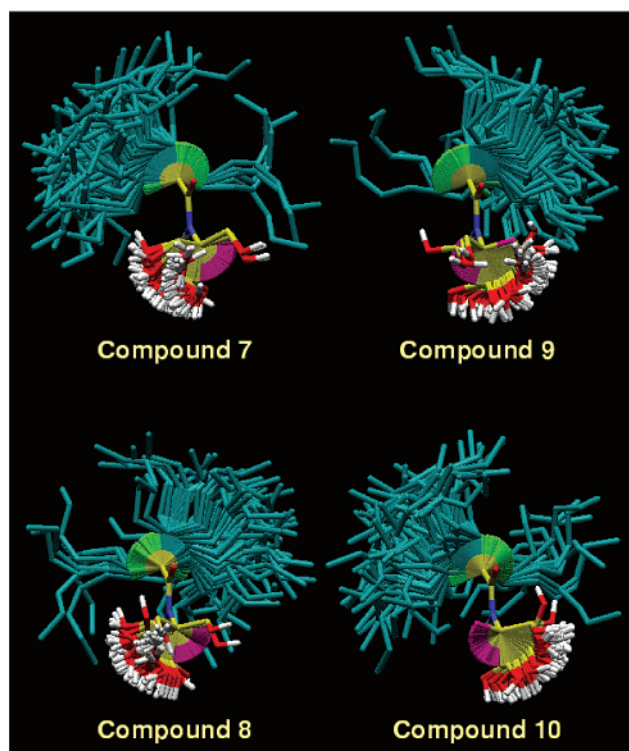

Figure 3. CM results in CHCl$_3$ for **7**−**10** are illustrated here. The headgroups of all 100 conformers of each compound superimposed at their amide groups are shown here. The methyl group at the C2 stereo center is colored green, while the C1′ stereo center methyl group is colored magenta. The acyl chains (colored cyan) have been truncated in order to simplify the display. The stereoisomeric pairs **7/9** and **8/10** are positioned with the amide group nearly perpendicular to the page and the amide oxygen pointing up. In this orientation, it is clear here that the C2 methyl (in green) and C1′ methyl (in magenta) groups can only populate a small portion of space and that the acyl chains (colored in cyan) have a preferred direction as they emerge from the headgroup.

chain, as some conformers had this segment oriented out of plane of the ligand body. This occurrence was presumably due to the proximity of the C2 and/or C1′ methyl groups in some conformations.

For **7** (C2 *R*; C1′ *R*) in CHC1$_3$, two major clusters were found. In one, the acyl chain adopts a near U-shaped conformation (33 members out of 100). In the other, the acyl chain of **7** is in an extended conformation (29 members out of 100). For **9** (C2 *S*; C1′ *S*), both U-shaped (43 members out of 100) and extended (29 members out
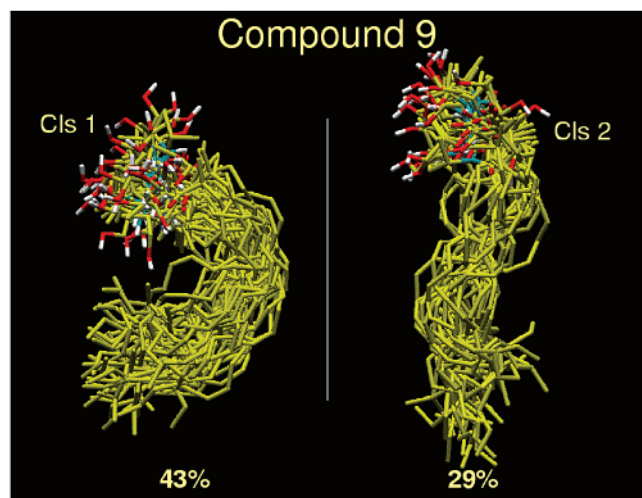
Figure 4. CM results in CHCl$_3$ are reported here for the major conformational families of **9**. Percentages reported are the percentage populations out of 100 conformers generated in the final phase of the CM calculation at 310 K.

of 100) conformational families were identified. For the **8/10** pair, 24 out of 100 (**8**) and 37 out of 100 (**10**) conformers were in a near U-shaped conformation, while 36 out of 100 (**8**) and 28 out of 100 (**10**) conformers were in an extended conformation. Figure 4 illustrates these results for **9**.

Endocannabinoid Interaction with the R* Form of CB1. The underlying hypothesis in the work described here is that while different agonist structures may occupy the same general binding site region (and therefore can displace each other in radioligand binding assays), the set of residues with which each structural class interacts may not be identical; therefore, structural overlap of all key regions between disparate structural classes is not a requirement in order for both classes of compounds to bind at CB1. As the result of this hypothesis, the focus in the present study was on the endocannabinoid SAR literature (i.e., acyl chain SAR and headgroup SAR).

CB1 Binding in the 7−10 Series. As presented in Figure 1, CM results for the acyl chain series of ethanolamides (**1−3** and **6**) suggested that higher CB1 affinity is associated with endocannabinoids that can form tightly curved structures. While there are no crystal structures of anandamide bound to CB1 available in the literature, there is an X-ray crystal structure of **1**'s parent acid, arachidonic acid (20:4, n-6) complexed with adipocyte lipid binding protein. In this structure, arachidonic acid clearly adopts a curved/U-shaped conformation.[20] We, therefore, hypothesized that a curved/U-shaped conformer may be the bioactive conformation for endocannabinoid ethanolamides at CB1. A conformer from this family of each of the ethanolamides **7−10** was used for docking studies in CB1 R*. As mutation studies have shown that K3.28(192) is crucial for the binding of anandamide at CB1[21] and SAR studies have shown that the C2′-hydroxyl group can be replaced with a methyl group with a slight enhancement in affinity,[22] we hypothesized that the amide oxygen, rather than the C2′ hydroxyl of anandamide and its analogues, interacts directly with K3.28(192). Each ligand was docked in a model of CB1 in its activated state (R*) because agonists are thought to have higher

affinity for the activated (R*) form of a G-protein-coupled receptor (GPCR) than for the inactive (R) form.[23] Each ligand was docked so that its carbonyl oxygen could hydrogen bond with K3.28(192). Figure 3 illustrates that keeping the carbonyl oxygen in a common orientation causes compounds **7−10** to have different spatial requirements for their headgroups. These requirements will influence how each conformer can dock with CB1 R*. The constraints on headgroup substituent positions (as illustrated in Figure 3) were then used as additional constraints in order to identify an initial docking position for each compound. Each ligand/CB1 R* complex was then minimized using the Amber* force field in Macromodel.[17]

The radius of curvature of each ligand acyl chain in the final energy-minimized bundle was assessed using the curvature analysis method described in the Materials and Methods section. These radii were 3.2 Å for **7**, 2.8 Å for **8**, 2.9 Å for **9**, and 2.9 Å for **10**. These radii are smaller than the average Cls 1 values for the 20:4, n-6 acyl chain of **1** (see Table 2), indicating that each analogue is tightly folded in the receptor binding pocket and undergoes additional compacting upon binding. It is interesting to note that the radius requirements imposed by the binding site for the lower affinity dimethyl analogues (**8−10**; 2.8−2.9 Å) result in acyl chain radii that fit within the lower end of the overall radii distribution in Figure 2 but are smaller than the smallest radii found for **1** itself (see 20:4, n-6 distribution in Figure 2). On the other hand, the radius of curvature imposed by the binding site for the high affinity dimethyl analogue (**7**; 3.2 Å) places the radius of **7** within the distribution of radii found for **1** (20:4, n-6 distribution in Figure 2).

Goutopoulos and co-workers found that **7** had a higher CB1 affinity (K_i = 7.42 nM) than its parent compound, anandamide (K_i = 78.2 nM), under the same assay conditions.[14] Figure 5 illustrates the results of the compound **7**/CB1 R* docking study. These results suggest reasons for the enhanced CB1 affinity of **7**. When the carbonyl oxygen of **7** interacts with K3.28, the C2 and C1′ methyl groups are positioned to "cup" V3.32-(196), forming a very good van der Waals interaction with this residue that "locks" the ligand in place. This is illustrated in the cut-out of Figure 5, which shows V3.32 (196) and **7** contoured at their Van der Waals (VdWs) radii. In addition, with the C1′ methyl in this position, the headgroup hydroxyl, is positioned to form an intramolecular hydrogen bond with the carboxamide oxygen as well. The ligand acyl chain is in a U-shaped conformation with a curvature radius of 3.2 Å. The aromatic amino acid side chains of F2.57(170) and F3.25(189) form C−H···π interactions with the C5−C6 and C11−C12 acyl chain double bonds, respectively, while other hydrophobic residues line the binding pocket in which the acyl chain is located, including L3.29(193), A7.36(380), M7.40(384), and L7.43(387).

Compounds **8−10** could be docked at CB1 using an acyl chain conformation from Cls 1 (U-shaped) and using the carboxamide oxygen/K3.28(192) interaction as well. However, no residues in the docked position were situated such that a very good VdWs interaction could take place with the C2 and C1′ methyl groups of these ligands nor were any hydrogen-bonding partners identi-
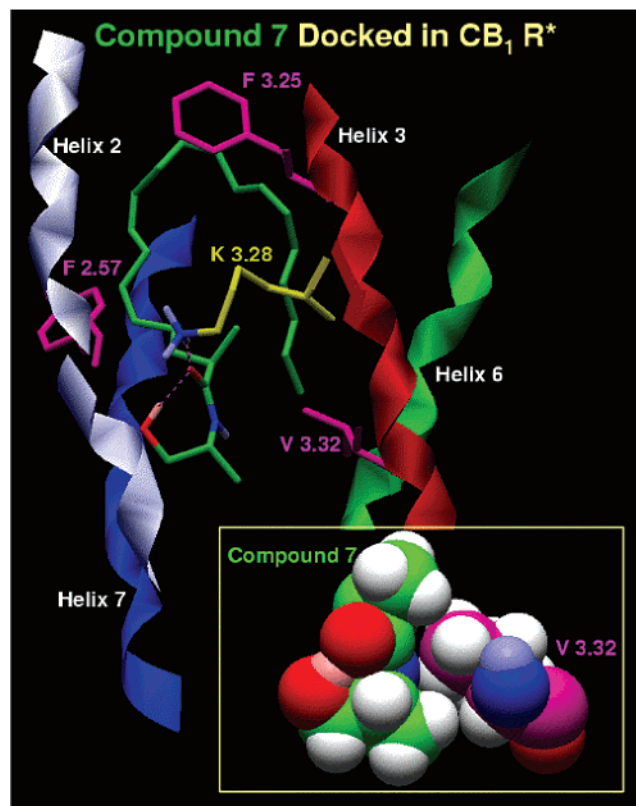
Figure 5. Results of the **7**/CB1 R* docking study are illustrated here. The amide oxygen of **7** interacts with K3.28-(192), while the C2 and C1′ methyl groups are positioned to "cup" V3.32(196), forming a very good van der Waals interaction with this residue that "locks" the ligand in place. This is illustrated in the cut-out, which shows V3.32(196) and **7** contoured at their Van der Waals (VdWs) radii. The headgroup hydroxyl is positioned to form an intramolecular hydrogen bond with the carboxamide oxygen as well. The ligand acyl chain is in a U-shaped conformation (acyl chain radius of curvature = 3.2 Å) corresponding to one of the major conformer clusters of **7** from CM calculations. The aromatic amino acid side chains of F2.57(170) and F3.25(189) interact with the C5−C6 and C11−C12 acyl chain double bonds, respectively.

fied for the headgroup hydroxyls in these ligands. This was true even for **8**, which has the same *R* stereochemistry at C1′ as **7**. The adjustments made by **8** because of the different stereochemistry at C2 force the molecule into a different headgroup conformation in order to maintain the K3.28(192) interaction. In this altered conformation, an intramolecular hydrogen bond cannot form due to poor hydrogen bond geometry. While **9** found no C−H⋯π interactions between aromatic residue side chains and its acyl chain, **8** (with F2.61(174) and F3.25(189)) and **10** (with F2.57(170)) did find such interactions.

Discussion

Endocannabinoid Interaction with the Cannabinoid CB1 Receptor. Consistency with Structural Data. One of the strengths of the CM method is that the conformational properties of a molecule can be fully characterized by the free energy of each of the conformations that it can adopt. This property includes not only the intrinsic energy of each conformational state but also the probability that the molecule will adopt each particular conformation relative to all other ones

accessible in an equilibrated thermodynamic ensemble.[15] Our previous CM study of arachidonic acid (20:4, n-6), the parent fatty acid of anandamide,[19] identified both extended and U-shaped conformers consistent with X-ray crystal structural data for arachidonic acid alone (extended/angle-iron)[24] and in complex (U-shaped).[20] Our CM results for rotation about each Csp^2-Csp^3 bond in the homoallylic portion of the arachidonic acid acyl chain revealed a broad range of populated torsion angle values from +60 to +180° and −60 to −180°, with maxima centered about +120 and −120°, respectively.[19] These results reflected the profound flexibility of the acyl chain in the homoallylic double-bond portion of the acyl chain and were consistent with results for arachidonic acid published by Rich,[25] who found that the barrier to rotation about the Csp^2-Csp^3 bond is ≤1.0 kcal/mol. In agreement with our earlier CM results, the acyl chain homoallylic double-bond portions of **1**−**3**, **6**, and **7**−**10** were found to be regions of high flexibility, leading each of these molecules to adopt both extended and U-shaped conformations, which have low free energies.

Our docking study of compounds **7**−**10** indicated that in **7**, an intramolecular hydrogen bond between the carboxamide oxygen and the headgroup hydroxyl was highly favored. This result is consistent with recent nuclear magnetic resonance (NMR) solution studies of anandamide reported by Bonechi and co-workers who found that an analogous intramolecular hydrogen bond in anandamide persists in solution.[26]

Consistency with Endocannabinoid SAR Data. The binding site interactions illustrated in Figure 5 are consistent with results first reported by Pinto and co-workers[22] who showed that the hydroxyl group in the headgroup region of anandamide could be replaced by a methyl group without a loss in CB1 affinity. In fact, a slight increase in CB1 affinity resulted from this substitution. This result suggested that the hydroxyl group is not essential for anandamide binding and also that this hydroxyl may exist in a hydrophobic region of CB1. This result has been echoed in later endocannabinoid SAR studies that show, for example, that a cyclopropyl headgroup results in a very high CB1 affinity ligand.[27] In the binding site identified for the endocannabinoids in Figure 5, the headgroup hydroxyl is located in a hydrophobic pocket. We have reported here that in **7**, the hydroxyl group can form an intramolecular hydrogen bond with the carboxamide oxygen, an interaction that is less possible or is impossible for **8**−**10** at the same site. The formation of such an intramolecular hydrogen bond in **7** helps the hydroxyl exist in a hydrophobic region and still satisfy a hydrogen bond. This may contribute to this ligand's enhanced affinity at CB1 relative to its congeners, **8**−**10**.

The endocannabinoid binding site model proposed here accounts for the endocannabinoid SAR requirement of at least three double bonds separated by methylene carbons with at least five saturated carbons in the tail.[10,11] It is clear from the CM results illustrated in Figure 1 that saturated regions of the acyl chain tend to prefer trans torsion angle conformations and, consequently, tend to be relatively extended, while the unsaturated (homoallylic double bond) portions of the acyl chain show a proclivity for curvature. As seen in

Figure 1 for the 20:3, n-6 (**2**); 20:4, n-6 (**1**); and 22:4, n-6 (**3**) ethanolamides, the molecules are capable of folding near the middle of the acyl chain because the last double bond in the acyl chains of these analogues occurs five carbons from the tail, placing the three or four homoallylic double bonds in the middle section of the acyl chain where they can produce curvature that results in a hairpin/J-shaped structure. It is interesting to note that Piomelli and co-workers hypothesized a similar folded conformation to be important for endocannabinoid interaction with another biological target, the anandamide transporter.[28] These investigators found a correlation between the end carbon to carboxamide carbon distance and transporter affinity in a series of endocannabinoid transporter analogues.

Consistency with CB1 Mutation Data. The binding site identified for the endocannabinoids in Figure 5 is consistent with the CB1 mutation literature that indicates that residue K3.28(192) is an important residue for the binding of anandamide (and also for the classical/nonclassical cannabinoids but not the aminoalkylindoles).[21] Song and Bonner reported that anandamide was unable to compete for [³H]WIN55,212-2 binding in a CB1 K3.28(192)A mutant and that the potency of anandamide in inhibiting adenosine cyclic 3′,5′-phosphate (cAMP) accumulation was reduced >100-fold. In Figure 5, the carboxamide oxygen of **7** is engaged in a hydrogen bond with K3.28(192). This hydrogen bond should be a very strong one because K3.28(192) is charged.[29]

Binding site interactions identified here for **7−10** are also consistent with the recent crystal structure of arachidonic acid bound to prostaglandin synthase.[30] This crystal structure shows several aromatic residues engaged in C−H···π interactions between aromatic ring hydrogens and double-bond π clouds along the acyl chain of arachidonic acid. In the CB1 binding site identified here (see Figure 5), the aromatic amino acid side chains of F2.57(170) and F3.25(189) interact, respectively, with the C5−C6 and C11−C12 acyl chain double bonds. Preliminary CB1 F3.25(189)A mutation studies support the participation of F3.25 in the anandamide binding site, as they indicate a 7-fold drop in anandamide's CB1 affinity upon a F3.25(189)A mutation.[31] The magnitude of affinity loss upon mutation to a nonaromatic residue is consistent with the loss of a C−H···π interaction, which is a moderate but nevertheless important interaction that contributes to protein stability.[32]

In Figure 5, V3.32(196) occupies the space between the C-1′ and C-2 methyl groups of **7** and is engaged in a hydrophobic interaction with these two methyl groups. As hydrophobic interactions are proportional to the amount of surface area in contact with each other (47 cal/mol Å², see ref 33), this interaction also contributes to the affinity of **7** for CB1.

Comparative Molecular Field Analysis (CoMFA) Models. The hypothesis that **1** adopts a folded/curved conformation in order to interact with the CB1 receptor has also been explored by other research groups in the generation of CoMFA models. Although CB1 CoMFA studies do not involve the presence of the 3D structure of the CB1 receptor and therefore cannot identify the specific amino acids with which the ligand interacts,

Chart 2
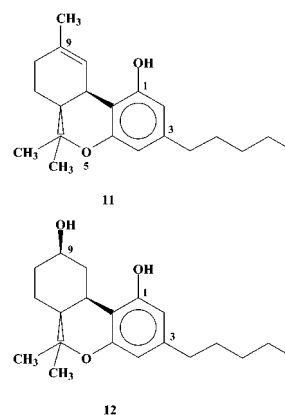
these studies do provide indirect information about the structural and electronic requirements for binding at this receptor and the relative positions of key regions of the receptor. In each of the CoMFA models, a classical cannabinoid was chosen as the template on which anandamide was superimposed. Thomas and co-workers[34] were first to report a CoMFA quantitative SAR (QSAR) pharmacophore model for anandamide and its analogues. These authors used constrained MD studies to explore conformations of **1** that present pharmacophoric similarities with the classical cannabinoid, Δ⁹-THC (**11**; Chart 2). A J-shaped or looped conformation of **1** was identified that had good molecular volume overlap with Δ⁹-THC (**11**) when (i) the carboxamide of **1** was overlaid with the pyran oxygen (O-5) in **11**; (ii) the headgroup hydroxyl of **1** was overlaid with the C-1 phenolic hydroxyl group of **11**; (iii) the five terminal carbons of the **1** fatty acid acyl chain were overlaid with the C-3 pentyl side chain of **11**; and (iv) the polyolefin loop of **1** was overlaid with the tricyclic ring system of **11**. These authors supported their use of a J-shaped conformation for **1** by citing synthetic results for the internal epoxidation undergone by peroxyarachidonic acid, which points to the J shape as necessary for such a reaction.

Tong and co-workers[35] reported a different pharmacophore model for **1** using constrained conformational searching and CoMFA. 9-Nor-9β-OH-HHC (**12**) was used as the template to which **1** and its analogues were fit. The conformation identified for **1** was a helical conformation in which (i) the oxygen of the carboxyamide overlaid the C-1 phenolic hydroxyl group of **12**; (ii) the headgroup hydroxyl overlaid the C-9 hydroxyl of **12**; (iii) the alkyl tail of **1** overlaid the C3 alkyl side chain of **12**; and (iv) the polyolefin loop overlaid the tricyclic ring structure of **12**. These authors supported their use of a helical-shaped **1** by citing a recent X-ray crystallographic structure, which shows that arachidonic acid adopts a helical conformation when it is a substrate for cyclooxygenase. The authors cite the close matching of common pharmacophoric elements of **1** and **12** as persuasive evidence of the biological relevance of this helical conformer.

CoMFA studies such as those cited above[34,35] require the choice of a template molecule and a hypothesized correspondence between key structural features of subject ligands. The underlying hypothesis in these superpositions is that anandamide and the template molecule occupy the same site at CB1 and therefore that

residues that interact with key functional groups on the template molecule will also interact with corresponding key regions in anandamide. Both the Thomas and the Tong CoMFA studies arrived at plausible, compact/folded (but different) conformations for anandamide. Both drew a structural correspondence between anandamide and classical cannabinoid compounds that are structurally divergent from the endocannabinoids. It is clear, however, that these two CoMFA studies are not in agreement with each other, as each adopts very different structural alignment rules with regard to the carboxamide oxygen and headgroup hydroxyl. Therefore, these two cannabinoid CoMFA models diverge from each other in the 3D position of key complementary receptor regions. In addition, because the focus of these studies was the development of a unified model (a classical/nonclassical/endocannabinoid CoMFA model), specific explanations, for example, for the relationship between the affinity and the number of acyl chain homoallylic double bonds were not sought.

As stated earlier in the Results section, the underlying hypothesis in the work described here is that while different agonist structures may occupy the same general binding site region (and therefore can displace each other in radioligand binding assays), the set of residues with which each structural class interacts may not be identical; therefore, structural overlap of all key regions between disparate structural classes is not a requirement in order for both classes of compounds to bind at CB1. As a result of this hypothesis, the focus in the present study was on the endocannabinoid SAR literature (i.e., acyl chain SAR and headgroup SAR). The CM method generated 100 low free energy structures of each compound at 310 K. In adopting this approach, we were able to consider all possible conformations for the endocannabinoids, rather than being confined to a smaller region of conformational space as is necessitated by working hypotheses of required overlap of key regions with a rigid template. We have reported previously that the transmembrane helix (TMH) 3−5−6−7 region of CB1 is the binding site for the nonclassical cannabinoid CP-55 940.[36] This study identified K3.28(192), W5.43(279), and N7.45(389) as hydrogen-bonding sites for the phenolic hydroxyl, northern aliphatic hydroxyl, and southern aliphatic hydroxyl of CP-55 940, respectively, and identified a group of hydrophobic amino acids (V6.43(351), L6.51(359), L7.41(385), and L7.44(388)) as the hydrophobic binding pocket for the CP-55 940 side chain. While this CP-55 940 binding site and that identified for **7** share only one direct interaction site in common (K3.28(192)), their binding sites sterically overlap in the TMH 3−7 region. These ligands, therefore, would be expected to displace one another in radioligand binding assays.

Finally, it is important to mention that the binding site model proposed here does not address one last aspect of endocannabinoid acyl chain SAR, the requirement for an acyl chain of 20−22 carbons. It is our hypothesis that this length requirement originates not from the requirements of the final binding site itself but from requirements for endocannabinoid entry into the binding pocket from lipid. We have recently shown that alkyl tail interaction with V6.43(351)/I6.46(354) (which forms a groove on CB1 TMH 6 into which an alkyl tail

can fit) results in the induction of an active state conformation for TMH 6.[37] Simulations of TMH 6/endocannabinoid interaction in a lipid environment are currently underway in our laboratory to test the hypothesis that only endocannabinoids with 20−22 carbon acyl chains (with at least three homoallylic double bonds and at least five saturated carbons at their ends) extend to the proper depth in the lipid membrane to access the V6.43/I6.46 groove.

Materials and Methods

Ligand Nomenclature. The acyl group in each of the ethanolamides studied here is designated using the accepted shorthand for long-chain unsaturated fatty acids. The acyl moiety 20:4, n-6 indicates the presence of a 20 carbon atom chain; four cis homoallylic double bonds, the first one of which is on the sixth carbon atom, counting from the noncarboxyl end of the acid.

Conformational Analysis. The CM technique[15] employs multiple Monte Carlo/simulated annealing (MC/SA) random walks using the MM3 force field and the generalized Born/surface area (GB/SA) continuum solvation model for chloroform as implemented in the Macromodel molecular modeling package.[17] CM conformational analyses were performed for the ethanolamides 22:4, n-6 (**3**); 20:4, n-6 (**1**); 20:3, n-6 (**2**); 20:2, n-6 (**6**); and for **7−10**. Calculations used $CHCl_3$ as solvent, because the binding site of the endocannabinoids is thought to be in the binding site crevice of the TMH bundle, a region that would not be expected to have a high dielectric. Each CM calculation was performed in two phases. In the exploratory phase, a random walk was used to identify the region of conformational space that is populated for each torsion angle studied. For molecules **1−3** and **6−10**, all torsion angles in the acyl chain for rotation about $C_{sp^3}-C_{sp^3}$ and $C_{sp^3}-C_{sp^2}$ bonds were allowed to vary. All torsion angles in the headgroup for rotation about $N_{sp^2}-C_{sp^3}$, $C_{sp^3}-C_{sp^3}$, and $C_{sp^3}-O_{sp^3}$ bonds in **7−10** were allowed to vary. The $C_{sp^2}-N_{sp^2}$ bond of the amide group was held fixed such that the amide group remained in a trans geometry. Starting at a temperature of 2070 K, 10 000 steps were applied to all rotateable bonds with cooling in 18 steps to a final temperature of 310 K. Trial conformations were generated at each temperature by randomly picking two torsion angles and changing each angle by a random value between ±180° and accepting or rejecting the resultant conformer using the Metropolis criterion. This calculation was repeated for a total of 100 cycles. "Memories" of values for each torsion angle that was accepted were used to map the conformational space.

In the biased-annealing phase of the calculation, only torsion angle moves that would keep the angle in "populated conformational space" were attempted. This phase began at a temperature of 722 K, cooling to 310 K in nine stages.

Finally, the output of 100 structures at 310 K was clustered using X-Cluster in Macromodel,[17] a program that reorders the structures according to their rms deviation and groups the structures into families of similar conformers. X-Cluster inputs the series of 100 conformations and computes the rms difference between all possible pairs of conformations. Structures 2−100 of the input sequence are then reordered on the basis of increasing rms deviation. In the new ordering, considering all 100 conformations, conformer 2 has the smallest rms deviation from conformer 1, and conformer 3 has the smallest rms deviation from conformer 2, etc. Because the conformations have been rearranged so that the rms deviation between nearest neighbors is minimized, any large jump in rms deviation between nearest neighbors is indicative of a large structural change and hence identifies a new conformational family or cluster. Because the structures are reordered based on the smallest rms deviation with the preceding structure, the same set of families emerge from the X-Cluster analysis no matter which conformer is first in the file.

Curvature Analysis. An adaptation of the fitting method of Kumar and Basal[38] originally designed for helix analysis was

employed here. To fit the acyl chains to a circle, a subset of atoms from two carbon atoms before the first C−C double bond to two carbon atoms after the last C−C double bond was chosen (e.g., C3−C17 in Chart 1, **1**). This same set of carbon atoms was used for the 22:4, n-6 (**3**); 20:3, n-6 (**2**); and 20:2, n-6 (**6**) analogues and for the docked structures of **7**−**10**. Bond midpoints between each pair of atoms were computed and fit to a circle of the form $(x - a)^2 + (y - b)^2 = r^2$, using a least squares procedure,[18] where point (a,b) is the center of the circle and r is its radius. Prior to the fitting procedure, a plane was chosen that minimized the distance of the points in the 3rd dimension from this plane. Subsequently, the points were rotated such that this plane coincided with the xy plane. In the case where a structure had atoms lying above or below the plane, these atoms were projected into the xy plane. Finally, for each conformation, these points were also fit to a straight line.

The rms deviation of the points from the best fit circle (RMSDC) and line (RMSDL) were obtained. On the basis of these data, the conformation was assigned to a circular structure (RMSDC < RMSDL and RMSDC < 0.8) or rejected as a circle. Conformations displaying linear geometry (RMSDL < RMSDC and the linear correlation coefficient > 0.8) were also rejected from the analysis. The average radii and standard deviation for the best fit circles are reported in Table 2. In the member's column, the number of structures in each Cls 1 family as identified by X-Cluster analysis of CM output is reported, followed by the number of conformations used in the curvature analysis (in parentheses).

The curvature analysis employed in the paper was meant to provide a two-dimensional (2D) measure of the overall gross structure present in the C3−C17 portion of the acyl chains of a given X-Cluster family. The first step in the curvature analysis of the cluster 1 (U/J-shaped families) involved the projection of all atoms into a plane. Most conformers analyzed were relatively 2D structures (i.e., near planar). In some cases, however, conformers were grouped in Cls 1 by X-Cluster whose head and tail segments bend toward each other, but whose central portions (C3−C17) were relatively straight, forming a C shape. These structures could not be fit to a circle in the C3−C17 region and were therefore removed from the set of conformers used to assess curvature in this region. The Cls 1, U/J-shaped families also included some more 3D conformers that had acyl chain ends that twisted out of the average plane of the backbone. Structures with such 3D features in the acyl tails cannot be adequately represented by points projected into a plane and therefore were removed from consideration as well. The number of such removed conformers varied with each analogue acyl chain studied but remained the minority of structures in every case.

Receptor Model Construction. Amino Acid Numbering System. In the discussion of receptor residues that follows, the amino acid numbering scheme proposed by Ballesteros and Weinstein is used.[39] In this numbering system, the most highly conserved residue in each TMH is assigned a locant of 0.50. This number is preceded by the TMH number and may be followed in parentheses by the sequence number. All other residues in a TMH are numbered relative to this residue. In this numbering system, for example, the most highly conserved residue in TMH 2 of the CB1 receptor is D2.50(163). The residue that immediately precedes it is A2.49(162).

R to R* Transition in GPCRs. Because agonists are thought to have higher affinity for the activated form of GPCRs,[23] agonist ligands in the work reported here were docked in a model of the activated state (R*) of CB1 (see below). This R* CB1 model was created by modification of our rhodopsin (Rho)-based model of the inactive (R) form of CB1 (see below) and guided by the biophysical literature on the R to R* transition. It has now been well-established in the biophysical literature that the R to R* transition in GPCRs is accompanied by significant changes in the TMH bundle (see refs 40 and 41 for reviews). These studies have indicated that activation of Rho is accompanied by a rigid domain motion of TMH 6 relative to TMH 3.[42] Lin and Sakmar[43] reported that

perturbations in the environment of W3.41 (along with W6.48) of Rho occur during the conformational change concomitant with receptor activation. This has been interpreted as originating from a counterclockwise rotation of TMH 3 and 6 (from an extracellular view). Jensen and co-workers[44] recently demonstrated through fluorescence studies in the β-2-adrenergic receptor that P6.50 in the highly conserved CWXP motif of TMH 6 can act as a flexible hinge that mediates the transition from R to R*. In the R state, these investigators propose that TMH 6 is kinked at P6.50 such that its cytoplasmic end is nearly perpendicular to the membrane and close to the cytoplasmic end of TMH 3. The transition to the R* state is accomplished by the straightening of TMH 6 such that the cytoplasmic part of TMH 6 moves away from the receptor core and upward toward the lipid bilayer.[44] Ballesteros and co-workers[45] recently proposed that a salt bridge between R3.50 and E6.30 at the intracellular end of the β-2-adrenergic receptor stabilizes this receptor in its inactive state. In their study of TMH 6 in the β-2-adrenergic receptor, Javitch and co-workers[46] documented that Cys 6.47 becomes available to the binding pocket only in a constitutively active β-2 mutant. The acquired accessibility of Cys 6.47 in the mutant was hypothesized to result from a rotation and/or tilting of the sixth membrane-spanning segment associated with activation of the receptor.

In the present study, the literature on GPCR activation discussed above was used to generate an R* CB1 TMH bundle from a model of the inactive (R) CB1 receptor based on the 2.8 Å crystal structure of Rho.[47] The creation of these two forms of CB1 is described below.

Model of Inactive (R) Form of CB1. A model of the inactive (R) form of CB1 was created using the 2.8 Å crystal structure of Rho.[47] First, the sequence of the human CB1 receptor[48] was aligned with the sequence of bovine Rho using the same highly conserved residues as alignment guides that were used initially to generate our first model of CB1.[49] TMH 5 in CB1 lacks the highly conserved proline in TMH 5 of Rho. The sequence of CB1 in the TMH 5 region was aligned with that of Rho as described previously[49] using its hydrophobicity profile. Helix ends for CB1 were chosen in analogy with those of Rho:[47] TMH 1, N1.28(112) − R1.61(145); TMH 2, R2.37(150) − H2.68(181); TMH 3, S3.21(185) − R3.56(220); TMH 4, T4.38(229) − C4.66(257); TMH 5, H5.34(270) − K5.64(300); TMH 6, R6.28(336) − K6.62(370); TMH 7, K7.32(376) − S7.57(401); and intracellular extension of TMH 7, D7.59(403) − C7.71(415). With the exception of TMH 1, these helix ends were found to be within one turn of the helix ends originally calculated by us and reported in 1995.[49] Changes to the general Rho structure that were necessitated by sequence divergences included the absence of helix-kinking proline residues in TMH 1 and TMH 5, the lack of a GG motif in TMH 2, and the presence of extra flexibility in TMH 6. Because TMH 6 figures prominently in the R to R* transition, we have studied the conformations accessible to TMH 6 in CB1 and CB2 using CM.[37] These studies revealed that TMH 6 in CB1 (but not CB2) has high flexibility due to the small size of residue 6.49 (a Gly) immediately preceding Pro 6.50. Two families of conformers were identified by CM for TMH 6 in CB1. Cluster 1 showed a pronounced proline kink (40 members out of 100, 71.2° average kink angle). Cluster 2 contained helices with less pronounced kinks (51 members out of 100, 30.1° average kink angle). A conformer from the more kinked CM family of CB1 TMH 6s (Cluster 1) was used in our model of the inactive (R) state of CB1. This conformer was selected (Pro kink angle = 53.1°) so that R3.50(214) and D6.30(338) could form a salt bridge at the intracellular ends of TMHs 3 and 6 in the CB1 TMH bundle. An analogous salt bridge has been shown to be an important stabilizer of the inactive state of the β-2-adrenergic receptor[45] and to be present in Rho.[47]

Model of Active (R*) Form of CB1. On the basis of experimental results for Rho and the β-2-adrenergic receptor,[42–46] the R* (active) CB1 bundle was created from the inactive (R) model of CB1 by rotating TMH 3 so that residue 3.41 changes environments.[43] This was accomplished by a 20°

counterclockwise (extracellular view) rotation of TMH 3 from its orientation in the inactive (R) bundle. In the R* bundle, a TMH 6 conformer from the second major conformational family (less kinked, 21.8° kink angle) identified by CM[37] was substituted for the TMH 6 conformer used in the inactive model of CB1. This conformer was chosen so that the salt bridge in the inactive state between R3.50(214) and D6.30(338) would be broken due to the movement of the intracellular end of TMH 6 away from that of TMH 3 and out into lipid.[45] TMH 6 was also rotated (counterclockwise from extracellular view) so that Cys 6.47 became accessible from inside the binding site crevice.[46]

Preparation of Helices. Each helix of the model was capped by acetamide at its N terminus and *N*-methylamide at its C terminus. Ionizable residues in the first turn of either end of the helix were neutralized, as were any lipid-facing charged residues. Ionizable residues were considered charged if they appeared anywhere else in the helix.

Ligand−Receptor Complex. CM results for each anandamide analogue (**7−10**) were used to identify an initial conformer for docking studies. A conformer from the curved/U-shaped cluster (Cls 1) of **7−10** (see Figure 4 for **9**) was selected and docked initially in CB1 R* using interactive computer graphics. The primary interaction site used in this docking was K3.28(192), which we have hypothesized interacts with the carboxamide oxygen of each derivative of **1** (see justification for this docking site in the Discussion section above). The range of headgroup substituent positions (as illustrated in Figure 3) were then used as additional constraints in order to identify an initial docking position for each ligand in the **7−10** series.

The energy of the CB1 R* TMH bundle/ligand complex was minimized using the AMBER* united atom force field in Macromodel 6.5 (Schrodinger Inc., Portland, OR). A distance-dependent dielectric, 8.0 Å extended nonbonded cutoff (updated every 10 steps), 20.0 Å electrostatic cutoff, and 4.0 Å hydrogen bond cutoff were used. The first stage of the calculation consisted of 2000 steps of Polak−Ribier conjugate gradient (CG) minimization in which a force constant of 225 kJ/mol was used on the helix backbone atoms in order to hold the TMH backbones fixed, while permitting the side chains to relax. The second stage of the calculation consisted of 100 steps of CG in which the force constant on the helix backbone atoms was reduced to 50 kJ/mol in order to allow the helix backbones to adjust. Stages one and two were repeated with the number of CG steps in stage two incremented from 100 to 500 steps until a gradient of 0.001 kJ/(mol Å ²) was reached.

References

(1) Devane, W. A.; Hanus, L.; Breuer, A.; Pertwee, R. G.; Stevenson, L. A.; Griffin, G.; Gibson, D.; Mandelbaum, A.; Etinger, A.; Mechoualn, R. Isolation and Structure of a Brain Constituent That Binds to the Cannabinoid Receptor. *Science* **1992**, *258*, 1946−1949.

(2) Smith, P. B.; Compton, D. R.; Welch, S. P.; Razdan, R. K.; Mechoulam, R.; Martin, B. R. The Pharmacological Activity of Anandamide, a Putative Endogenous Cannabinoid, in Mice. *J. Pharmacol. Exp. Ther.* **1994**, *270*, 219−227.

(3) Showalter, V. M.; Compton, D. R.; Martin, B. R.; Abood, M. E. Evaluation of Binding in a Transfected Cell Line Expressing a Peripheral Cannabinoid Receptor (CB2): Identification of Cannabinoid Receptor Subtype Selective Ligands. *J. Pharmacol. Exp. Ther.* **1996**, *278*, 989−999.

(4) Hanus, L.; Gopher, A.; Almog, S.; Mechoulam, R. Two New Unsaturated Fatty Acid Ethanolamides in Brain That Bind to the Cannabinoid Receptor. *J. Med. Chem.* **1993**, *36*, 3032−3034.

(5) Mechoulam, R.; Ben-Shabat, S.; Hanus, L.; Ligumsky, M.; Kaminski, N. E.; Schatz, A. R.; Gopher, A.; Almog, S.; Martin, B. R.; Compton, D. R.; Pertwee, R. G.; Griffin, G.; Bayewitch, M.; Barg, J.; Vogel, Z. Identification of an Endogenous 2-Monoglyceride, Present in Canine Gut, That Binds to Cannabinoid Receptors. *Biochem. Pharmacol.* **1995**, *50*, 83−90.

(6) Hanus, L.; Saleh, A.-L.; Fride, E.; Breuer, A.; Vogel, Z.; Shaley, D. E.; Kustanovich, I.; Mechoulam, R. 2-Arachidonyl Glyceryl Ether, an Endogenous Agonist of the Cannabinoid CB1 Receptor. *Proc. Natl. Acad. Sci. U.S.A.* **2001**, *98*, 3662−3665.

(7) Breivogel, C. S.; Selley, D. E.; Childers, S. R. Cannabinoid Receptor Agonist Efficacy for Stimulating [35 S]GTPγS Binding to Rat Cerebellar Membranes Correlates with Agonist-Induced Decreases in GDP Affinity. *J. Biol. Chem.* **1998**, *273*, 16865−16873.

(8) Piomelli, D.; Beltramo, M.; Glasnapp, S.; Lin, S. Y.; Goutopoulos, A.; Xie, X.-Q.; Makriyannis, A. Structural Determinants for Recognition and Translocation by the Anandamide Transporter. *Proc. Natl. Acad. Sci. U.S.A.* **1999**, *96*, 5802−5807.

(9) Cravatt, B. F.; Giang, D. K.; Mayfield, S. P.; Boger, D. L.; Lerner, R. A.; Gilula, N. B. Molecular Characterization of an Enzyme that Degrades Neuromodulatory Fatty-Acid Amides. *Nature* **1996**, *384*, 83−87.

(10) Reggio, P. H.; Traore, H. Conformational Requirements for Endocannabinoid Interaction with the Cannabinoid Receptors, the Anandamide Transporter and Fatty Acid Amidohydrolase. *Chem. Phys. Lipids* **2000**, *108*, 15−35.

(11) Palmer, S. L.; Khanolkar, A. D.; Makriyannis, A. Natural and Synthetic Endocannabinoids and Their Structure−Activity Relationships. *Curr. Pharm. Des.* **2000**, *6*, 1381−1397.

(12) Sheskin, T.; Hanus, L.; Slager, J.; Vogel, Z.; Mechoulam, R. Structural Requirements for Binding of Anandamide-type Compounds to the Brain Cannabinoid Receptor. *J. Med. Chem.* **1997**, *40*, 659−667.

(13) Abadji, V.; Lin, S.; Taha, G.; Griffin, G.; Stevenson, L. A.; Pertwee, R. G.; Makriyannis, A. (*R*)-Methanandamide; a Chiral Novel Anandamide Possessing Higher Potency and Metabolic Stability. *J. Med. Chem.* **1994**, *37*, 1889−1893.

(14) Goutopoulos, A.; Fan, P.; Khanolkar, A. D.; Xie, X.-Q.; Lin, S.; Makriyannis, A. Stereochemical Selectivity of Methanandamides for the CB1 and CB2 Cannabinoid Receptors and Their Metabolic Stability. *Bioorg. Med. Chem.* **2001**, *9*, 1673−1684.

(15) Guarnieri, F.; Weinstein, H. Conformational Memories and the Exploration of Biologically Relevant Peptide Conformations: An Illustration for the Gonadotropin-Releasing Hormone. *J. Am. Chem. Soc.* **1996**, *118*, 5580−5589.

(16) Karplus, M.; Petsko, G. A. Molecular Dynamics Simulations in Biology *Nature* **1990**, *347*, 631−639.

(17) Mohamadi, F.; Richards, N. G. J.; Guida, W. C.; Lizkamp, R.; Lipton, M.; Caulfield, C.; Chang, G.; Hendickson, T.; Still, W. C. Macromodel-An Integrated Software System for Modeling Organic and Bioorganic Molecules Using Molecular Mechanics. *J. Comput. Chem.* **1990**, *11*, 440−467.

(18) Minitab Statistical Software, version 13; Minitab Inc.: State College, PA; http://www.minitab.com.

(19) Barnett-Norris, J.; Guarnieri, F.; Hurst, D. P.; Reggio, P. H. Exploration of Biologically Relevant Conformations of Anandamide, 2-Arachidonylglycerol and Their Analogues Using Conformational Memories. *J. Med. Chem.* **1998**, *41*, 4861−4872.

(20) Lalonde, J. M.; Levenson, M. A.; Roe, J. H.; Bernlohr, D. A.; Banaszak, L. J. Adipocyte Lipid-Binding Protein Complexed with Arachidonic Acid. *J. Biol. Chem.* **1994**, *269*, 25339−25347.

(21) Song, Z. H.; Bonner, T. I. A Lysine Residue of the Cannabinoid Receptor is Critical for Receptor Recognition by Several Agonists, but not WIN-55, 212. *Mol. Pharmacol.* **1996**, *49*, 891−896.

(22) Pinto, J.; Potie, F.; Rice, K. C.; Boring, D.; Johnson, M. R.; Evans, D. M.; Wilken, G. H.; Cantrell, C. H.; Howlett, A. C. Cannabinoid Receptor Binding and Agonist Activity of Amides and Esters of Arachidonic Acid. *Mol. Pharmacol.* **1994**, *46*, 516−522.

(23) Leff, P. The Two-State Model of Receptor Activation. *Trends Pharmacol. Sci.* **1995**, *16*, 89−97.

(24) Ernst, J.; Sheldrick, W. S.; Fuhrhop, J. H. The Structure of the Essential Unsaturated Fatty Acids. Crystal Structure of Linoleic Acid and Evidence for the Crystal Structures of α-Linolenic and Arachidonic Acid. *Z. Naturforsch.* **1979**, *346*, 706−711.

(25) Rich, M. R. Conformational Analysis of Arachidonic and Related Fatty Acids Using Molecular Dynamics Simulation. *Biophys. Acta* **1993**, *1178*, 87−96.

(26) Bonechi, C.; Brizzi, A.; Brizzi, V.; Francoli, M.; Donati, A.; Rossi, C. Conformational Analysis of N-arachidonylethanolamide (Anandamide) Using Nuclear Magnetic Resonance and Theoretical Calculations. *Magn. Reson. Chem.* **2001**, *39*, 432−437.

(27) Hillard, C. J.; Manna, S.; Greenberg, M. J.; Dicamelli, R.; Ross, R. A.; Stevenson, L. A.; Murphy, V.; Pertwee, R. G.; Campbell, W. B. Synthesis and Characterization of Potent and Selective Agonists of the Neuronal Cannabinoid Receptor (CB1). *J. Pharmacol. Exp. Ther.* **1999**, *289*, 1427−1433.

(28) Piomelli, D.; Beltramo, M.; Glasnapp, S.; Lin, S. Y.; Goutopoulos, A.; Xie, X.-Q.; Makriyannis, A. Structural Determinants for Recognition and Translocation by the Anandamide Transporter. *Proc. Natl. Acad. Sci. U.S.A.* **1999**, *96*, 5802−5807.

(29) Fersht, A. R.; Shi, J.-P.; Knill-Jones, J.; Lowe, D. M.; Wilkinson, A. J.; Blow, D. M.; Brick, P.; Carter, P.; Waye, M. M. Y.; Winter, G. Hydrogen Bonding and Biological Specificity Analyzed by Protein Engineering. *Nature* **1985**, *314*, 235−238.

(30) Malkowski, M. G.; Ginell, S. L.; Smith, W. L.; Garavito, R. M. The Productive Conformation of Arachidonic Acid Bound to Prostaglandin Synthase. *Science* **2000**, *289*, 1933−1937.

(31) McAllister, S.; Hurst, D. P.; Reggio, P. H.; Abood, M. Unpublished results.

(32) Brandl, M.; Weiss, M. S.; Jabs, A.; Söhnel, J.; Hilgenfeld, R. C−H···π Interactions in Proteins. *J. Mol. Biol.* **2001**, *307*, 357−377.

(33) Sharp, K. A.; Nicholls, A.; Fine, R. F.; Honig, B. Reconciling the Magnitude of the Microscopic and Macroscopic Hydrophobic Effects. *Science* **1991**, *252*, 106−109.

(34) Thomas, B. F.; Adams, I. B.; Mascarella, S. W.; Martin, B. R.; Razdan, R. K. Structure−Activity Analysis of Anandamide Analogues: Relationship to a Cannabinoid Pharmacophore. *J. Med. Chem.* **1996**, *39*, 471−479.

(35) Tong, W.; Collantes, E. R.; Welsh, W. J.; Berglund, B. A.; Howlett, A. C. Derivation of a Pharmacophore Model for Anandamide Using Constrained Conformational Searching and Comparative Molecular Field Analysis. *J. Med. Chem.* **1998**, *41*, 4207−4215.

(36) Tao, Q.; McAllister, S. A.; Andreassi, J.; Nowell, K. W.; Cabral, G. A.; Hurst, D. P.; Bachtel, K.; Ekman, M. C.; Reggio, P. H.; Abood, M. E. Role of a Conserved Lysine in the Peripheral Cannabinoid Receptor (CB2): Evidence for Subtype Specificity. *Mol. Pharmacol.* **1999**, *55*, 605−613.

(37) Barnett-Norris, J.; Hurst, D. P.; Buehner, K.; Ballesteros, J. A.; Guarnieri, F.; Reggio, P. H. Agonist Alkyl Tail Interaction with Cannabinoid CB1 Receptor V6:43/I6.46 Groove Induces a Helix 6 Active Conformation. *Int. J. Quantum Chem.* **2002**, *88*, 76−86.

(38) Kumar, S.; Bansal, M. Structural and Sequence Characteristics of Long Alpha Helices in Globular Proteins. *Biophys. J.* **1996**, *71*, 1574−1586.

(39) Ballesteros, J. A.; Weinstein, H. Integrated Methods for the Construction of Three-Dimensional Models and Computational Probing of Structure Function Relations in G Protein-Coupled Receptors. In *Methods in Neuroscience*; Conn, P. M., Sealfon, P. M., Eds.; Academic Press: San Diego, 1995; Vol. 25, Chapter 19, pp 366−428.

(40) Hulme, E. C.; Lu, Z.-L.; Ward, S. D. C.; Allman, K.; Curtis, C. A. M. The Conformational Switch in 7-Transmembrane Receptors: The Muscarinic Receptor Paradigm. *Eur. J. Pharmacol.* **1999**, *375*, 247−260.

(41) Sansom, M. S.; Weinstein, H. Hinges, Swivels and Switches: The Role of Prolines in Signaling via Transmembrane Alpha-Helices. *Trends Pharmacol. Sci.* **2000**, *21*, 445−51.

(42) Farrens, D. L.; Altenbach, C.; Yang, K.; Hubbell, W. L.; Khorana., H. G. Requirement of Rigid-Body Motion of Transmembrane Helicies for Light Activation of Rhodopsin. *Science* **1996**, *274*, 768−770.

(43) Lin, S. W.; Sakmar, T. P. Specific Tryptophan UV-Absorbance Changes Are Probes of the Transition of Rhodopsin to its Active State. *Biochemistry* **1996**, *35*, 11149−11159.

(44) Jensen, A. D.; Guarnieri, F.; Rasmussen, S. G. F.; Asmar, F.; Ballesteros, J. A.; Gether, U. Agonist-Induced Conformational Changes at the Cytoplasmic Side of TMH 6 in the β_2 Adrenergic Receptor Mapped by Site-Selective Fluorescent Labeling. *J. Biol. Chem.* **2001**, *276*, 9279−9290.

(45) Ballesteros, J. A.; Jensen, A. D.; Liapakis, G.; Rasmussen , S. G.; Shi, L.; Gether, U.; Javitch, J. A. Activation of the Beta 2-Adrenergic Receptor Involves Disruption of an Ionic Lock Between the Cytoplasmic Ends of Transmembrane Segment 3 and 6. *J. Biol. Chem.* **2001**, *276*, 29171−29177.

(46) Javitch, J. A.; Fu, D.; Liapakis, G.; Chen, J. Constitutive Activation of the β_2 Adrenergic Receptor Alters the Orientation of Its Sixth Membrane-Spanning Segment. *J. Biol. Chem.* **1997**, *272*, 18546−18549.

(47) Palczewski, K.; Kumasaka, T.; Hori, T.; Behnke, C. A.; Motoshima, H. B. A.; Fox, B. A.; LeTron, I.; Teller, D. C.; Okada, T.; Stenkamp, R. E.; Yamamoto, M.; Miyano, M. Crystal Structure of Rhodopsin: A G-Protein-Coupled Receptor. *Science* **2000**, *289*, 739−745.

(48) Gerard, C. M.; Mollereau, C.; Vassart, G.; Parmentier, M. Molecular Cloning of a Human Brain Cannabinoid Receptor Which is Also Expressed in Testis. *Biochem. J.* **1991**, *279*, 129−134.

(49) Bramblett, R. D.; Panu, A. M.; Ballesteros, J. A.; Reggio, P. H. Construction of a 3D Model of the Cannabinoid CB1 Receptor: Determination of Helix Ends and Helix Orientation. *Life Sci.* **1995**, *56*, 1971−1982.